Sensors and Actuators A 323 (2021) 112638

Contents lists available at ScienceDirect

Sensors and Actuators A: Physical

journal homepage: www.elsevier.com/locate/sna

Inkjet printing of multi-stripes based deflection monitoring sensor on flexible substrate

Saleem Khan*, Shawkat Ali, Arshad Khan, Moaaz Ahmed, Bo Wang, A. Bermak

Division of Information and Computing Technology, College of Science and Engineering, Hamad Bin Khalifa University, Qatar Foundation, Doha, Qatar

ARTICLE INFO

Article history:
Received 20 October 2020
Received in revised form 27 January 2021
Accepted 18 February 2021
Available online 26 February 2021

Keywords:
Printing
Strain/Deflection sensors
Polymer
Nanoparticles
Nanocomposites

ABSTRACT

This work presents an interesting approach towards rapid manufacturing of multi-stripes based deflection sensors developed through printing technologies. The deflection sensor is made of multiple small-scale strain sensing stripes sandwiched between consecutive conducting stripes. The drop-on-demand inkjet printing is used to pattern silver (Ag) nanoparticles ink as conducting interconnects and metallic stripes, whereas the piezoresistive sensing layer is obtained by mixing powdered carbon black and MWNTs in PDMS base matrix, resulting into a conducting nanocomposite. Different physical, optical, electrical, and adhesion-loss tests were performed as evaluation of the printing experiments. Deflection sensing was evaluated by mounting the sensors on opening cover-head of a plastic box to monitor different opening angles. Four detection angles at 0°, 10°, 45° and 90° were evaluated, for which the sensor showed prominent response at each level. The plastic box was used to represent the fill levels of a waste collection bin. The sensors will be advanced further by making an array of sensors where other parameters such as temperature, humidity, and concentration of the VOCs can also be monitored. All these advancements will be headed towards smart waste collection that is an integral part of Smart Cities development as well as internet-of-things (IoT) applications.

1. Introduction

Printed electronics on unconventional substrates are growing swiftly, while new exciting applications are emerging as the technology heads toward maturity [1–6]. Printing is an additive manufacturing technology used to deposit solution-based materials in less processing steps on diverse planar and nonplanar substrates [2,7–10]. The substrative procedures in standard clean room processes involve more material wastage, increased manufacturing time and are restricted to the use of finely polished substrates such as electronic grade Silicon (Si) wafers [7,8,11]. As against the multi-steps' silicon micromachining, the direct printing of functional materials on target substrates simplifies the process, minimize the fabrication time and cost as well as reducing the material wastage [1,12,13]. Various printing techniques have evolved in-line with the rapid growth of printed and flexible electronics [14–18]. All these methods are distinguished based on the operating principle, process-ability of materials with different rheological properties i.e. viscosities, surface tension and potentially on the desired feature sizes on the target substrates [1,7,8,11]. Recently, many proof of concept devices have been developed with a special focus on sensors' applications [19–25]. Among these, the piezoresistive based strain sensors for deflection or deformation measurements are widely explored by utilizing combination of multiple materials for synthesis of conductive nanocomposites [19,20,26–29].

Piezoresistance is interesting for many applications especially for monitoring of deflections resulting from tensile stress and strain [30–33]. Conventionally, metallic strain gauges with varying resistances as well as solid-state semiconductor devices with changing mobilities against strain are used for piezoresistance based sensors [31,34]. However, these devices are limited to certain shapes and applications, and cannot be applied onto nonplanar surfaces in a conformable fashion. Further, these materials and structures have low gauges factors making it challenging for a wide range of deflection sensing applications [34–36]. Therefore, polymer based conductive nanocomposites are considered the most suitable alternative to address these issues and have thus been explored by many researchers especially in the context of printed sensors [30,36,37]. Most of the piezoresistive nanocomposite materials are engineered and synthesized by mixing conductive nanofillers in an elastomeric matrix [35,37–40]. They are mechanically flexible and stretchable maintaining the electrical properties when mounted on uneven surfaces and are bound to repeatable relaxation and

* Corresponding author.
E-mail address: sakhan3@hbku.edu.qa (S. Khan).

https://doi.org/10.1016/j.sna.2021.112638
0924-4247/

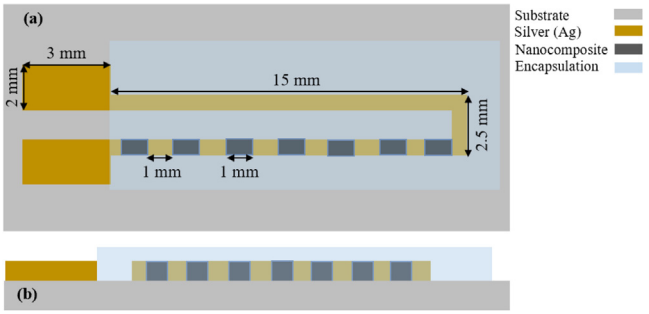

Fig. 1. Design of multi-stripes based deflection sensor, (a). Top View, (b) cross-sectional view.

contraction movements [31,34]. The change in bulk resistance as a result of external applied force is used to determine the tensile strain or level of deflection [36]. Conducting nanofillers make micron-scaled interconnecting threads or contacting point within the elastomeric matrix and percolation mechanism causes change the resistance against external stresses and strains [31,41]. The elastomeric based nanocomposites are capable of sustaining large strains without significant loss in the physical texture and have thus found attractions in highly sensitive strain related applications [42,43]. Although these polymer nanocomposites have the challenges of non-linearity, hysteresis, and temperature drifts, they are effective for large strains, simple and cost-effective to fabricate [34,35,44]. These advantages make them a better choice of sensing elements for applications requiring complaint integration of materials.

A new approach towards rapid manufacturing of a deflection sensor is proposed in this research based on multi-stripes of a conductive and nanocomposite materials. Combination of each stripe work as an individual strain sensor and the piezoresistive materials is sandwiched between two metallic contacts in a coplanar fashion. Inkjet printing is adopted for printing the metallic interconnections, pads, and stripes. Blade casting is used to deposit the nanocomposite material. Silver (Ag) nanoparticles' based ink (obtained from ANP inks) is printed using inkjet system. A combination of MWNTs (multiwall carbon nanotubes) and carbon black ink are mixed in PDMS (polydimethylsiloxane) base matrix. Different mixing ratios were used to optimize the sensor performance. The nanocomposite is deposited through a hard mask prepared in a thin plastic sheet using blade casting technique. Different physical, optical, electrical and piezoresistive sensing performances are evaluated in planar as well as in bent conditions.

2. Materials and methods

2.1. Design

Designing multi-stripes based strain sensor allows for rapid detection of longitudinal changes occurring in a structure. Each stripe works as a localized strain sensor and combination of multiple stripes form an array that enables covering large area of strain. The piezoresistive stripes are sandwiched between consecutive conducting bands, which enhances the performance of overall sensor and amplify the detection especially for the structures bending at multiple angles and at different joints. The alternate combination of multiple sensing stripes is useful for large area coverage. Data from the individual sensing stripe subjected to deflect is passed on to the contacting pads through neighboring conducting band and unobstructed sensing stripe. This would ultimately help in reducing the conduction losses as well as the response time of the sensor that might be occurring in large area structures. Fig. 1(a and b) shows schematics of the top and cross-sectional views of the proposed strain sensor. Length of the sensor is kept at 15 mm connected by pads, whereas length and width of each sensing stripe is 1 mm correspondingly.

2.2. Substrates

Substrates play significant role in the design of printing experiments and their selection is primarily based on the target application determined by the physical, thermal, mechanical, and electrical properties. Polymer substrates are the most suitable as they are lightweight, conformable, cost-efficient, and ideal for wearable and portable applications [12]. Glass transition temperature (Tg) is one of the most important parameters to be considered for adopting polymer-based substrates for printed electronics. Tg of the substrates determines the thermal budget of the whole manufacturing process and therefore selection of all the constituent materials and processes for a device are reliant on the polymer substrate [1]. This research employs cellulose mixed polymer substrates i.e. Clarifoil obtained from Celanese (UK). The 50 μm thick substrate with Tg of 140 °C, surface energy ~42 dyn/cm, transparency 91 %, specific gravity of 1.32 and surface roughness of ~10 nm (rms), was selected for the printing experiments. Substrate were cleaned with deionized (DI) water followed by a dehydration step. A UV ozone treatment was performed for 3 min before printing experiments.

2.3. Electrodes materials

The electrical conducting patterns are developed by using Ag nanoparticles based solution. Ag ink especially developed for inkjet printing was purchased from ANP (DGP 40LT-15C) and used without any further modifications. Ag nanoparticles loading of ~38 % in ethylene glycol is at the right viscosity range i.e. ~10 cP required for drop on demand inkjet system.

2.4. MWNT/Carbon/PDMS nanocomposite

The nanocomposite solution was synthesized by mixing MWNTs (multiwall carbon nanotubes, product no. 412,988), Carbon black (product No. 699,624) and PDMS (polydimethylsiloxane) (Dow SYLGARD 140) matrix. Incorporating only MWNTs in PDMS require higher concentrations of the conductive fillers, which are more challenging for printing processes. A low percolation threshold is desired to retain the static as well as dynamic mechanical, physical and electrical properties of MWCNT/PDMS composites. Uniform dispersion of nanofillers is of prime importance and contributes mainly to performance of the sensors. Therefore, to enhance the solubility and reduce MWNTs content in PDMS, carbon black ink was used as a precursor. Powdered carbon black purchased from Sigma Aldrich and mixed in chloroform at ~10 wt.%. The solution was stirred manually and for uniform dispersion, solution was sonicated at a frequency of 40 kHz for 30 min. MWNTs purchased from Sigma Aldrich having outer diameters of 6–9 nm, length 5 μm and ~2.5 g/mL density at room temperature. MWNTs (at 5 wt. %) were also dispersed in chloroform through mechanical stirring and kept in ultrasonic bath at frequency 40 kHz for 30 min. After uniform dispersions, both the solutions of carbon and MWNTs were mixed at 2:1 respectively. Further, PDMS (Dow Corning Sylgard 184) was mixed with the prepared solution followed by mechanical stirring for 10 min. Composite solution was kept again in ultrasonic bath at 40 kHz for 3 h. Cross-linking agent was added in 10:1 into the composite and degassed completely in a desiccator. After degassing steps, nanocomposites were printed at the desired positions using a blade casting procedure. Schematics in Fig. 2 show the process flow of synthesizing nanocomposite solution.

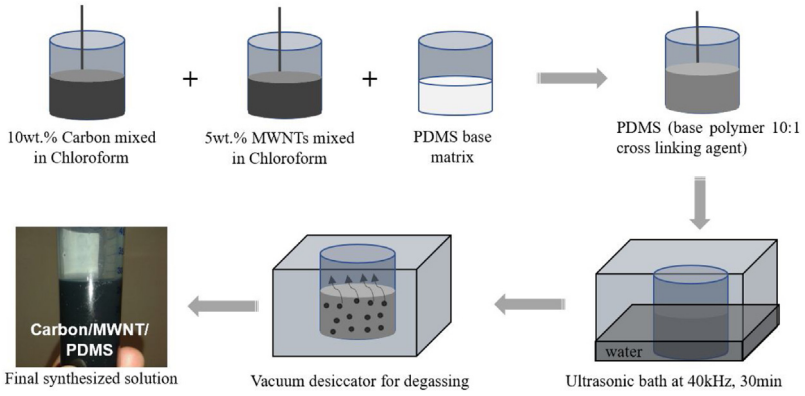

Fig. 2. Steps for synthesizing nanocomposite material.

3. Printing experiments

3.1. Inkjet printing of Ag

Ag nanoparticles ink was used to print the electrical interconnections, pads and conducting stripes using piezoelectric actuation based Dimatix 2850, Inkjet printing system. Dimension of the interconnections, sensing stripes and inter-stripes spacing were experimentally validated and the optimized designs were selected. To maintain the electrical conductivity under bending conditions, width of the interconnections and sensing stripes were kept at 1 mm. A 10 pL nozzle printhead was used for the Ag printing. Substrates were properly cleaned, and surface activated before printing. Deionized (DI) water was used to clean the substrate, followed by drying using nitrogen. UV (ultraviolet) ozone treatment of 3 min was performed after dehydration step. This time was optimized experimentally by changing the treatment time and observing the corresponding print quality. Important printing parameters such as jetting waveform, drop velocity (at 7 mm/sec), platen temperature (45 °C), jet frequency at 2 kHz, print standoff from platen at 500um, and drop-to-drop spacing of 25 μm were optimized and selected in the Dimatix drop manager software. Three layers were deposited to increase layer thickness. This contributes significantly to enhancing the electrical conductivity as well as the mechanical robustness and adhesion of the Ag patterns to the target substrate. The final step of drying the ink was performed in an oven at 100 °C for 4 h. The increased time is sufficient to produce stronger adhesion and electrical conductivity.

3.2. Printing nanocomposite

The inter-stripes' spacing of printed Ag was filled with carbon/MWNTs/PDMS-based nanocomposite using the doctor blade coating technique. The substrate was treated again with UV ozone after completing the sintering of Ag patterns. This allows to surface modification of the substrate resulting into uniform dispersion and strong adhesion of the nanocomposite material on the target substrate. As the nanocomposite is more viscous as compared to the Ag solution, a hard mask with corresponding opening for the stripes at desired spacings is used for the patterned deposition. A laser scribing tool was used to prepare the hard mask in a thin sheet of plastic. Thickness of the plastic sheet determines the deposition of sufficiently thick layer of the nanocomposite. Therefore, to achieve sufficient thickness and easy processability, 150 μm thick plastic sheet was selected for the hard mask. Internal sides of shadow mask openings were lubricated with petroleum jelly that makes the lift-off easier after the drying step. A moderately warm platen (i.e. 50 °C) is desirable for uniform distribution as well as rapid evaporation of the residual solvents. Two coating cycles were executed at an inter-layer delay of 10 min. The samples were kept at 70 °C for 2 h as a partial curing step. This allowed the safe removal of the masking sheet before keeping the samples for complete polymerization of the PDMS at 90 °C overnight. An encapsulation layer by using only a thin layer PDMS is applied. ZIF (zero insertion force) connectors were used to connect to the pads for the signal readout.

4. Results and discussion

The printed Ag conducting patterns as well sensing piezoresistive layers were characterized to determine the different physical, electrical, and electro-mechanical properties required for the reliable performance of a strain sensor. In case of Ag patterns, the uniformity, layer thickness, and adhesion-loss tests are of prime importance for the electrical conductivity and reliability of the printed patterns on polymer substrates. Profilometry, adhesion and performance of nanocomposite stripes is also determined at different orientations. Finally, the piezoresistive response of the sensors is checked at different angular deflections on practical applications. Results based on the physical characteristics and responses with both materials are investigated and discussed in the following sub-sections

4.1. Sheet Resistance of the conductive patterns

Sheet resistance of the Ag patterns is important be to be measured both in planar and in bent mode. As the sensor is aimed to be deployed on a bending or deflecting objects, therefore any drop in the electrical conductivity during varying conditions need to be pre-determined. Four-point collinear probe (Weistron) system was applied utilizing high impedance voltmeter for current and voltage analysis (configuration shown in inset of Fig. 3). The probes are equally spaced, where the outer two probes are used to source current while the inner two probes are used to measure the voltage drop across the test sample area. The sheet resistance measured both in the planar and bent (50 mm diameter) showed no significant difference. The sheet resistance values obtained i.e. ~ 13.2–13.8 Ω/sq, are in the close ranges as provided by the supplier i.e. 11–12 Ω/sq. Fig. 3 shows results of the sheet resistance in planar and bent mode.

4.2. Optical characterization and adhesion-loss test

Optical characterizations of the printed Ag and nanocomposite layers were performed using optical microscope as well as SEM (scanning electron microscope). It is important to observe the print quality and uniformity of the printed structures. Fig. 4(a–c) shows

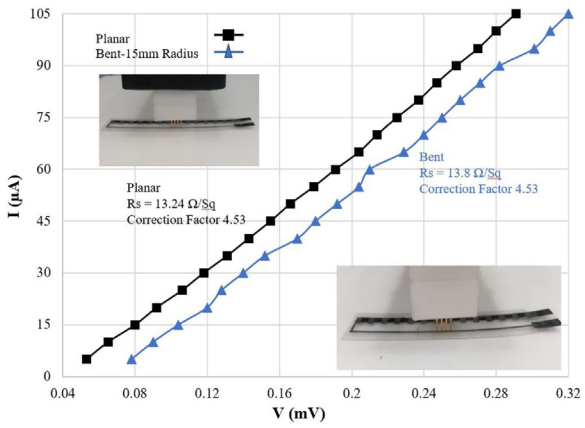

Fig. 3. Sheet resistivity in planar and bent mode (radius 25 mm) of substrate.

optical micrograph of the printed sensing structures, SEM images of Ag and carbon/MWNTs/PDMS nanocomposite, respectively. It is clear from the SEM images that a very uniform layer of the Ag patterns is obtained, as the ink is comprised of single type of material with uniform average size of the Ag nanoparticles. A uniform agglomeration of these nanoparticles is desired after complete sintering, which is ideal for better performance of the sensing devices. Nearly uniform distribution of the nanofillers is obtained for the nanocomposite layer as shown in Fig. 4(c). Micron-scaled agglomeration sites of the carbon/MWNTs at random positions within the PDMS matrix are observed, showing increased contacting channels for the electrical conduction within the PDMS bulk. Thickness of both Ag and nanocomposite layers are determined by using a mechanical profilometer. The three inkjet printing cycles produced approximately 1 μm thicker layer, whereas the nanocomposite layer thickness is about 50 μm. Optical 3-D Nano-Profiler is used for the surface morphology. Ag is observed to have very smooth surface as obvious from the uniformly dispersed nanoparticles solution as well as from the ideal printing conditions. The surface roughness for Ag observed is about 20 nm RMS (root mean square). On the other side, the nanocomposite layer surface is more rougher as also can be seen in the SEM image of Fig. 4, and this is due to the agglomeration peaks occurring from the MWCNTs. An approximate value for the surface roughness observed for multiple nanocomposite layers is in the range of 450–500 nm (RMS). These values are acceptable and are observed to have least effect on the sensor performance.

The adhesion-loss test was performed at multiple orientations by using standard peel-off test. The tests were performed at different stages i.e. in planar mode and after multiple bending cycles. No adhesion-loss in the Ag patterns were observed before and after executing the bending cycles. However minor detachment of the nanofillers is observed from the top surface of the nanocomposite layer. The bulk layer remained firmly in contact with the substrate without any significant degradation or cracks in the physical structure of the nanocomposite layer. This measurement was repeated for more than hundred bending cycles resulting into no delamination of any of the printed layers.

4.3. Electrical conductance of the combined stripes

Electrical conductance of the whole structure is of particular interest as the percolation threshold of the nanofillers is tuned based on the electrical response of printed nanocomposite layer. The effective utilization of these nanocomposites for sensors and conductive structures is governed by their actuation mechanism that is based on the quantity, orientation and conductive channels generated by the nanofillers in the polymer matrix. The electrical conductance is often modeled by considering the filler resistance (R_f) and the contact resistance (R_C) as described by Eq. 1. The contact resistance in turn is contributed by the constriction resistance (R_{CR}) through the small area between fillers and the tunneling resistance (R_T) between thin polymeric layers or surfactant coating on the conductive fillers. Fig. 5 shows the trending line of increasing nanofiller concentration, where a critical threshold value is needed to acquire sufficient conductive channels within the bulk matrix. The percolation threshold is the minimum required filler concentration at which, besides the establishment of sufficient conductive channels, mechanical properties of the matrix materials are also retained. Concentrations (i.e. 10 and 5 wt.%) used in this research were selected based on the experimental outcome of the electrical as well as mechanical properties of the nanocomposite layer. Sensors were tested in planar as well as deflection modes for electrical conductivity measurements. Fig. 6 shows graph of the resistance response of the sensor when placed on a planar surface as well as bent in a concave fashion at an angle of 70°. A source meter is used to record the resistance variations in the sensors both in planar and bent conditions. The base resistance is stabilized by placing the sensor on a planar surface for 125 s, and it is clear from the graph (Fig. 6) that very less variation is occurring until the sensor

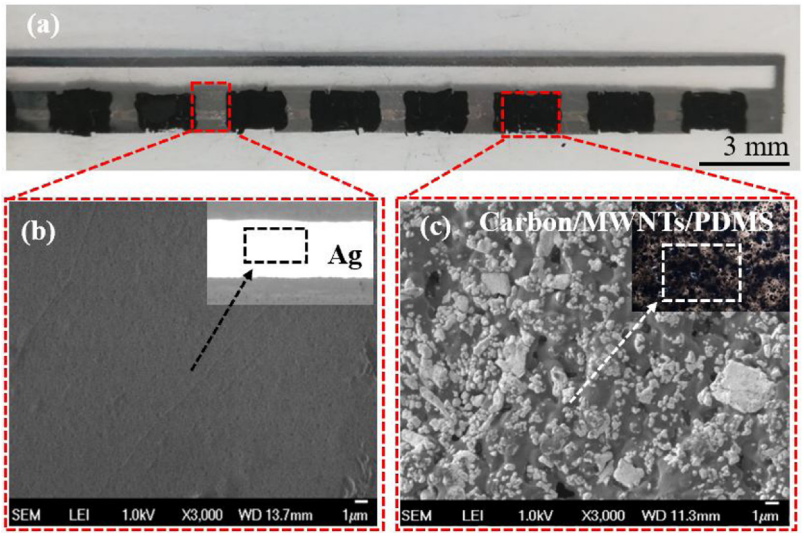

Fig. 4. (a) Optical micrograph of the strain sensor, (b). SEM of Ag layer, (c) SEM of Carbon/MWNTs/PDMS printed layer.

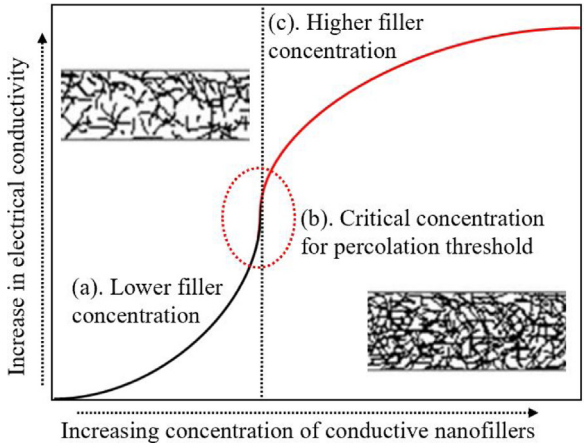

Fig. 5. Electrical conductivity of conductive composites as a function of filler fraction, where "*a*, *b*, *c*" denote the corresponding conductivities against nanofillers concentration within the polymeric matrix.

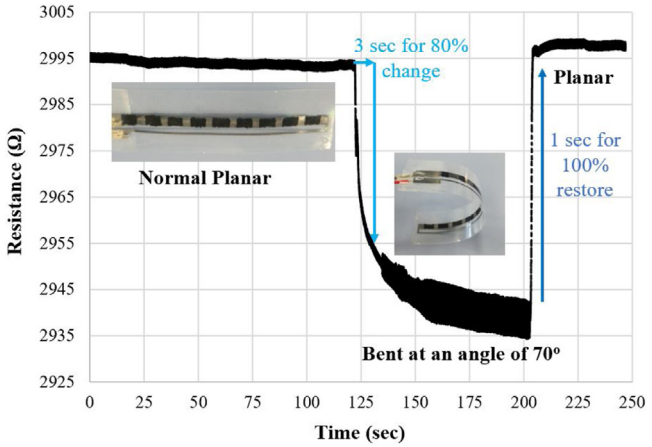

Fig. 6. Resistance change at planar and bent mode at an angle of 70O.

is bent at an angle of 70°. Resistance of the sensor decreases from 2.995 kΩ to 2.935 kΩ as the sensor is deflected in a concave fashion partly due to the compressed conductive nanofillers enhancing further the conducting channels within the matrix. Significant variation of 60 Ω in the base resistance of the sensor at 70° deflection is sufficient enough to monitor minute deflections. Responsivity of the sensor (shown in Fig. 6) is monitored for more than 80 % variation in the base resistance that is reached within a short period of 3 s. This deflection is made gradually and stopped after reaching at an angle of approximately 70°. However, the restoration to initial values is very abrupt and the base resistance is reached within 1 s as soon as the sensor is released to the normal planar position. No hysteresis is observed, and the initial resistance values are restored within 2 s making the sensor highly responsive to angular deflections. The elastomeric property of PDMS offers slight deformation after compressing or stretching the bulk layer within the elastic limits of PDMS. The change in bulk resistance due to this percolation mechanism can be exploited for piezoresistive related actions, where the applied force or elastic strain is correlated with resistance variations. The sensor is further evaluated for deflection at various angles by using a custom made setup (shown in the inset of Fig. 7). Both ends of the sensor were fixed in the clamps of the setup to allow the deflection at central part of the sensor patch while electrically connected to the sourcemeter. Effective length of the sensor is 15 mm and the system is deflected at various angles ranging from 0° to 90°. Resistance of the sensor is measured at each incremental angle of 15O/step, as shown in Fig. 7. The change in resistance is almost linear as seen in Fig. 7 (a) with respect to the corresponding angular deflection. Resolution of the sensor approximated in this configuration to about 0.85 Ω/θ°. Fig. 7(b) shows the sensitivity graph, determined from the measurements acquired for angular deflection shown in Fig. 7(a). The data presented in Fig. 7(a) is observed to be repeatable without any significant variations when the sensor is tested for at least twenty times. The error bars show the accuracy level of the sensor when tested at corresponding angle twenty times each. This showed a minimum variation of about ±1Ω randomly at each recorded value. This variation however might be due to the physical handling of the sensor and gradual change of the deflection angle manually. This could further be improved if an automated system is used where abrupt change in the angular deflection is made possible. Hysteresis in the sensor response is also evaluated by bending and releasing at the same rate and angular deflection as shown in graph of Figs. 8 and 9. Comparing the corresponding values at each angular deflection, it is observed that a negligible amount of hysteresis is present in the resistance response of the sensor (approximately 1Ω), which again could possibly be due to the manual handling of the sensor for angular deflection.

$$R_{Total} = R_f + R_{CR} + R_T \quad (1)$$

4.4. Deployment on objects

Sensor was deployed on the opening cover of a closed box to demonstrate the practical application. Placement of the sensors on small box is aimed to investigate the different opening conditions of a box head-cover. As the sensors are partly planned for

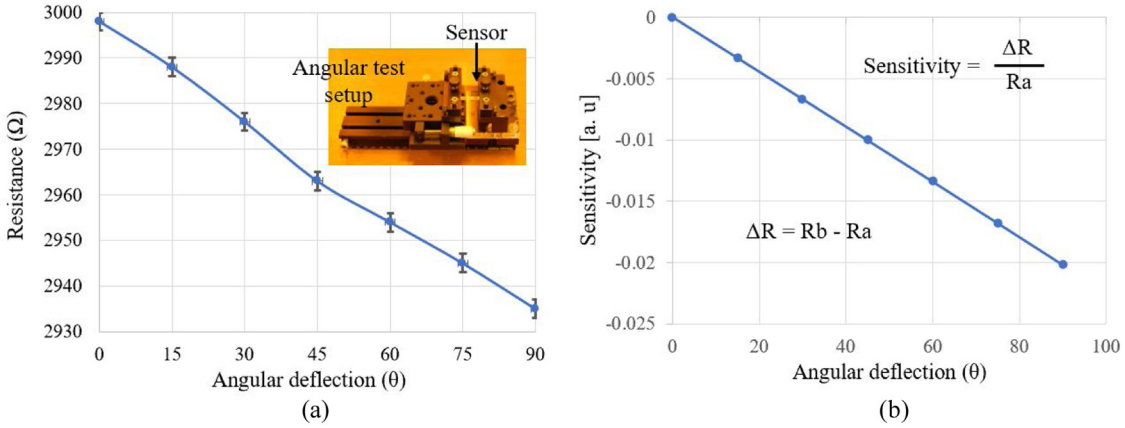

Fig. 7. (a) Sensor response in terms of resistance variation against various angular deflections and testing 20 times each at corresponding angle, (b) Sensitivity of the sensor.

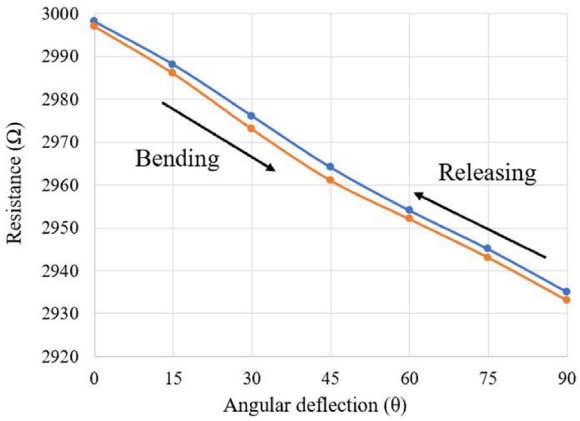

Fig. 8. Hysteresis evaluation for complete bending and releasing cycle of the sensor.

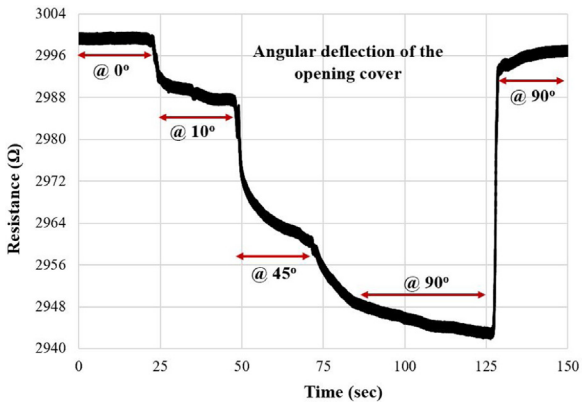

Fig. 10. Resistance response of the sensor to different angular orientations of the head-cover.

development of a smart waste collection bin, where the sensors will be installed to monitor the fill level of the container. Different opening scenarios of the box's head-cover are considered in this investigation. The analogy is based on different conditions, keeping in mind the different fill levels of the waste bin. For instance, the unfilled condition is determined by reading the base resistance of the deflection sensor. A small angular deflection i.e. 10° upwards by the opening cover is considered initial alarming signal of the fill condition. Further deflection of about 45°, show completely filled condition, whereas a deflection of 90° is considered overfilled condition. Figs. 8 and 9 shows all these four states of the head-cover by using a small, closed box for lab level tests. The sensor was deployed on the permanently locked side of the box and one side is free to deflect upon opening of the head-cover. The corresponding resistance responses were recorded by using Keithly sourcemeter. The sensor is attached such that one side is fixed and other end is free to move with the changing position of the opening cover. Configuration and orientation of the sensor is against the orientation of the opening cover. When the head-cover is at an angle of 90°, the sensor deflection is at 0°, whereas at the closed head-cover position, the sensor deflects at 90°. Fig. 10 shows graph of the resistance responses at each angular deflection considered in this study. A prominent variation of 13Ω and 60Ω were recorded both for the minimum deflection of 10° as well as for the 90° orientation, respectively. Considering the changing climatic conditions, especially the warm conditions of Gulf countries, the sensors were tested within the range of 25−50 °C. Fig. 11 shows temperature response for the four different measuring tests performed on the same sensor sample. The change in temperature variation is in very close range for all the four tests. An average change in resistance variation of 13 Ω in the bulk is recorded against a temperature rise from 25 °C to 50 °C. This temperature response needs to be adjusted or filtered out

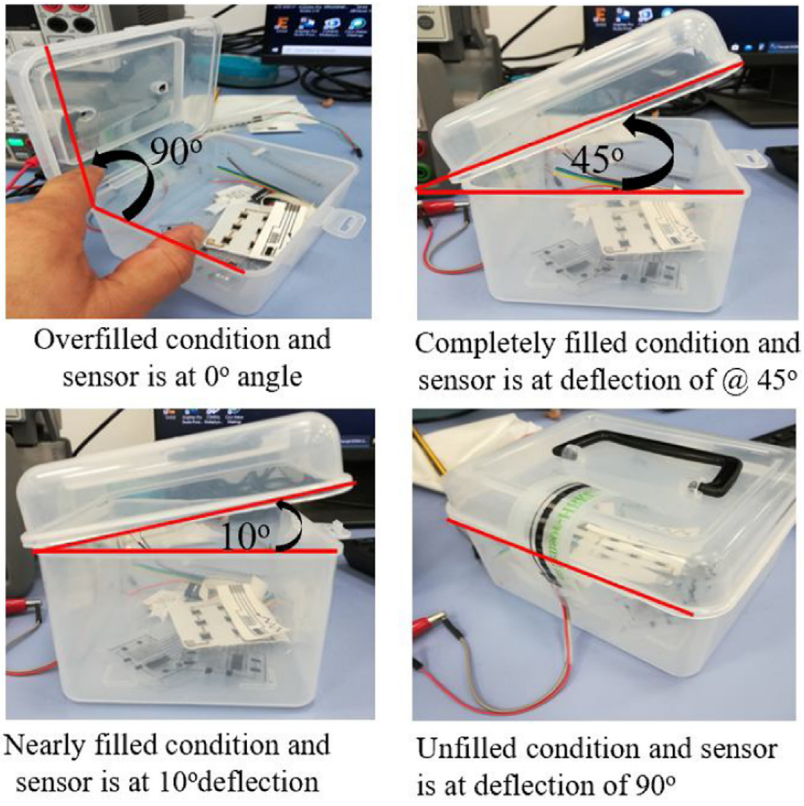

Fig. 9. Different fill scenarios of the small box head-cover.

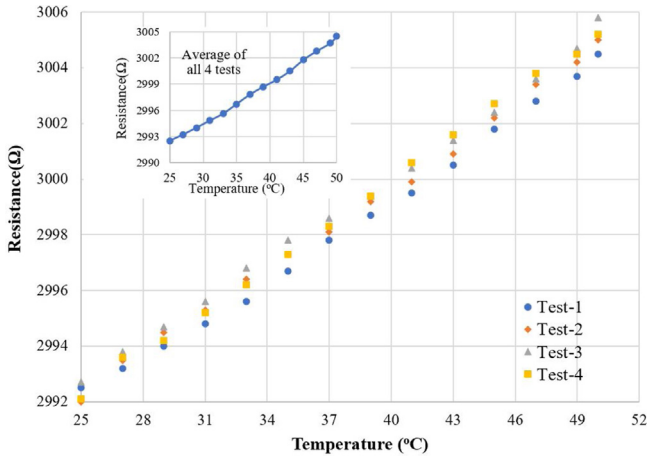

Fig. 11. Temperature response of the Sensor at four different test sets.

while monitoring the fill condition of the waste bin placed in outdoor environment. One possible solution is to use the same type of sensor explicitly for temperature monitoring. The increase in resistance due to temperature rise will be added as an offset value and subtracted from each corresponding resistance value of the fill level monitoring sensor.

5. Conclusion and future work

Multi-stripes based deflection sensor is presented in this research for monitoring of wide range of angular orientations. The nanocomposite material obtained from mixing of carbon black, MWNTs and PDMS is sandwiched between Ag conductive bands in a coplanar fashion. Each stripe works as a discrete strain sensor, which is ideal for applications exposed to uneven tensile strain or deflections at multiple joining points. The physical, optical, and electrical properties of the sensor were evaluated. The adhesion-loss test performed in the planar as well as bend conditions showed a strong adhesion of the printed materials to the polymer substrate. Electrical properties of the metallic patterns were also evaluated in planar and bent modes to make sure; these structures do not contribute in the piezoresistance response of the sensor. Finally, the sensors were mounted on a plastic box to represent a waste collection bin, where the various fill-level scenarios such as filled and overfilled conditions were investigated. The sensor can detect the deflection caused by opening of the head-cover at minimum angle as 10° and maximum at 90° at which the head-cover is completely flipped up. The presented results are very promising for deployment of deflection sensor on large area surfaces for real-time monitoring of strain related activities. The sensors will be advanced further by making an array of different sensors, where other parameters such as temperature, humidity, and concentration of the VOCs (volatile organic compounds) can also be monitored in a waste bin. All these advancements will be headed towards smart waste collection methods that is an integral part of Smart Cities development as well as IoT (internet of things) applications.

Declaration of Competing Interest

All the authors contributed equally and declare no conflict of interest.

Acknowledgement

This work was supported by NPRP from the Qatar National Research Fund (a member of Qatar Foundation) under Grant NPRP10-0201-170315 and NPRP11S-0110-180246.

References

[1] S. Khan, L. Lorenzelli, R.S. Dahiya, Technologies for printing sensors and electronics over large flexible substrates: a review, IEEE Sensors J. 15 (2015) 3164–3185.
[2] R.R. Søndergaard, M. Hösel, F.C. Krebs, Roll-to-Roll fabrication of large area functional organic materials, J. of Polymer Sci. Part B: Polymer Phys. 51 (2013) 16–34.
[3] A. Nag, S.C. Mukhopadhyay, J. Kosel, Wearable flexible sensors: a review, IEEE Sens. J. 17 (2017) 3949–3960.
[4] S. Khan, S. Ali, A. Bermak, Recent developments in printing flexible and wearable sensing electronics for healthcare applications, Sensors 19 (2019) 1230.
[5] L. Nayak, S. Mohanty, S.K. Nayak, A. Ramadoss, A review on inkjet printing of nanoparticle inks for flexible electronics, J. Mater. Chem. C 7 (2019) 8771–8795.
[6] T. Stockinger, B. Liedl, M. Steiner, R. Schwödiauer, F. Padinger, S. Bauer, et al., Printed sensors on paper and wood—the frugal way of in-line detection to characterize the crosslinking behaviour of water-based glues, Sens. Actuators B Chem. 324 (2020) 128750.
[7] T. Seifert, E. Sowade, F. Roscher, M. Wiemer, T. Gessner, R.R. Baumann, Additive manufacturing technologies compared: morphology of deposits of silver ink using inkjet and aerosol jet printing, Ind. Eng. Chem. Res. 54 (2015) 769–779.
[8] J. Oliveira, V. Correia, H. Castro, P. Martins, S. Lanceros-Mendez, Polymer-based smart materials by printing technologies: improving application and integration, Addit. Manuf. 21 (2018) 269–283.
[9] H.D. Goldberg, R.B. Brown, D.P. Liu, M.E. Meyerhoff, Screen printing: a technology for the batch fabrication of integrated chemical-sensor arrays, Sens. Actuators B Chem. 21 (1994) 171–183.
[10] D. Maddipatla, B.B. Narakathu, M. Atashbar, Recent progress in manufacturing techniques of printed and flexible sensors: a review, Biosensors 10 (2020) 199.
[11] M. Singh, H.M. Haverinen, P. Dhagat, G.E. Jabbour, Inkjet printing—process and its applications, Adv. Mater 22 (2010) 673–685.
[12] Y. Khan, A. Thielens, S. Muin, J. Ting, C. Baumbauer, A.C. Arias, A new frontier of printed electronics: flexible hybrid electronics, Adv. Mater. 32 (2020) 1905279.
[13] V. Beedasy, P.J. Smith, Printed electronics as prepared by inkjet printing, Materials 13 (2020) 704.
[14] M. Gao, L. Li, Y. Song, Inkjet printing wearable electronic devices, J. Mater. Chem. C 5 (2017) 2971–2993.
[15] N. Yogeswaran, W. Dang, W.T. Navaraj, D. Shakthivel, S. Khan, E.O. Polat, et al., New materials and advances in making electronic skin for interactive robots, Adv. Robot. 29 (2015) 1359–1373.
[16] S. Khan, S. Ali, A. Bermak, Smart manufacturing technologies for printed electronics, in: Hybrid Nanomaterials-Flexible Electronics Materials, IntechOpen, 2019, ed:.
[17] M.V. Kulkarni, S.K. Apte, S.D. Naik, J.D. Ambekar, B.B. Kale, Ink-jet printed conducting polyaniline based flexible humidity sensor, Sens. Actuators B Chem. 178 (2013) 140–143.
[18] D. Maddipatla, B.B. Narakathu, M. Ochoa, R. Rahimi, J. Zhou, C.K. Yoon, et al., Rapid prototyping of a novel and flexible paper based oxygen sensing patch via additive inkjet printing process, RSC Adv. 9 (2019) 22695–22704.
[19] Y. Shu, C. Li, Z. Wang, W. Mi, Y. Li, T.-L. Ren, A Pressure sensing system for heart rate monitoring with polymer-based pressure sensors and an anti-interference post processing circuit, Sensors 15 (2015) 3224–3235.
[20] R. Dahiya, W.T. Navaraj, S. Khan, E.O. Polat, Developing electronic skin with the sense of touch, Frontline Technology (2015).
[21] S. Khan, L. Lorenzelli, R. Dahiya, Flexible MISFET devices from transfer printed Si microwires and spray coating, IEEE J. Electron Devices Soc. 4 (2016) 189–196.
[22] T. Sekine, R. Sugano, T. Tashiro, J. Sato, Y. Takeda, H. Matsui, et al., Fully printed wearable vital sensor for human pulse rate monitoring using ferroelectric polymer, Sci. Rep. 8 (2018) 4442.
[23] S. Ali, S. Khan, A. Bermak, All-printed human activity monitoring and energy harvesting device for Internet of Thing applications, Sensors 19 (2019) 1197.
[24] T. Beduk, E. Bihar, S.G. Surya, A.N. Castillo, S. Inal, K.N. Salama, A paper-based inkjet-printed PEDOT: PSS/ZnO sol-gel hydrazine sensor, Sens. Actuators B Chem. 306 (2020) 127539.
[25] F.J. Romero, A. Rivadeneyra, A. Salinas-Castillo, A. Ohata, D.P. Morales, M. Becherer, et al., Design, fabrication and characterization of capacitive humidity sensors based on emerging flexible technologies, Sens. Actuators B Chem. 287 (2019) 459–467.
[26] S. Khan, S. Tinku, L. Lorenzelli, R.S. Dahiya, Flexible tactile sensors using screen-printed P (VDF-TrFE) and MWCNT/PDMS composites, IEEE Sensors J. 15 (2015) 3146–3155.
[27] C.-W. Lai, S.-S. Yu, 3D printable strain sensors from deep eutectic solvents and cellulose nanocrystals, ACS Appl. Mater. Interfaces 12 (2020) 34235–34244.
[28] R. Xie, Y. Xie, C.R. López-Barrón, K.-Z. Gao, N.J. Wagner, Ultra-stretchable conductive iono-elastomer and motion strain sensor system developed therefrom, Technol. Innov. 19 (2018) 613–626.
[29] Y.-Q. Li, P. Huang, W.-B. Zhu, S.-Y. Fu, N. Hu, K. Liao, Flexible wire-shaped strain sensor from cotton thread for human health and motion detection, Sci. Rep. 7 (2017) 45013.

[30] H. Zhao, J. Bai, Highly sensitive piezo-resistive graphite nanoplatelet-carbon nanotubes hybrids/polydimethylsilicone composites with improved conductive network construction, ACS Appl. Mat. & Interfaces (2015).
[31] R.M. Mutiso, K.I. Winey, Electrical properties of polymer nanocomposites containing rod-like nanofillers, Prog. in Polymer Sci. 40 (2015) 63–84.
[32] S. Stassi, V. Cauda, G. Canavese, C.F. Pirri, Flexible tactile sensing based on piezoresistive composites: a review, Sensors 14 (2014) 5296–5332.
[33] S. Ali, A. Hassan, S. Khan, A. Bermak, Flexible coplanar waveguide strain sensor based on printed silver nanocomposites, SN Applied Sciences 1 (2019) 744.
[34] M. Haghgoo, M. Hassanzadeh-Aghdam, R. Ansari, A comprehensive evaluation of piezoresistive response and percolation behavior of multiscale polymer-based nanocomposites, Compos. Part A Appl. Sci. Manuf. 130 (2020) 105735.
[35] S. Khan, L. Lorenzelli, Recent advances of conductive nanocomposites in printed and flexible electronics, Smart Mater. Struct. 26 (2017) 083001.
[36] H. Hwang, Y. Kim, J.H. Park, U. Jeong, 2D percolation design with conductive microparticles for low-strain detection in a stretchable sensor, Adv. Funct. Mater. 30 (2020) 1908514.
[37] L. Gao, C. Zhu, L. Li, C. Zhang, J. Liu, H.-D. Yu, et al., All paper-based flexible and wearable piezoresistive pressure sensor, ACS Appl. Mater. Interfaces 11 (2019) 25034–25042.
[38] Y. Wei, S. Chen, F. Li, K. Liu, L. Liu, Hybrids of silver nanowires and silica nanoparticles as morphology controlled conductive filler applied in flexible conductive nanocomposites, Composites Part A: Appl. Sci. and Manufac. 73 (2015) 195–203.
[39] S. Khan, W. Dang, L. Lorenzelli, R. Dahiya, Flexible pressure sensors based on screen printed P(VDF-TrFE) and P(VDF-TrFE)/MWCNTs, IEEE Trasac. on Semicond. Manufact 28 (2015), p. In Press.
[40] S. Khan, L. Lorenzelli, R. Dahiya, Bendable piezoresistive sensors by screen printing MWCNT/PDMS composites on flexible substrates, 2014 10th Conference on Ph. D. Research in Microelectronics and Electronics (PRIME) (2014) 1–4.
[41] M.F. Clayton, R.A. Bilodeau, A.E. Bowden, D.T. Fullwood, Nanoparticle orientation distribution analysis and design for polymeric piezoresistive sensors, Sens. Actuators A Phys. 303 (2020) 111851.
[42] M. Xu, F. Li, Z. Zhang, T. Shen, J. Qi, Piezoresistive sensors based on rGO 3D microarchitecture: coupled properties tuning in local/integral deformation, Adv. Electron. Mater. 5 (2019) 1800461.
[43] S.J.K. O'Neill, H. Gong, N. Matsuhisa, S. Chen, H. Moon, H.C. Wu, et al., A carbon flower based flexible pressure sensor made from large-area coating, Adv. Mater. Interfaces (2020) 2000875.
[44] N. Afsarimanesh, A. Nag, S. Sarkar, G.S. Sabet, T. Han, S.C. Mukhopadhyay, A review on fabrication, characterization and implementation of wearable strain sensors, Sens. Actuators A Phys. (2020) 112355.

Biographies

Saleem Khan received his Ph.D. in Materials Science Engineering from University of Trento, Italy, and master's degree in Electronic Engineering from Jeju National University, South Korea. He worked as a Scientific Collaborator at EPFL, Switzerland and is currently a Postdoc fellow at HBKU, Qatar Foundation, Qatar. He has more than nine years of experience in exploring printable materials and printing technologies. His research activities are focused on development of all–printed microelectronic transducers and sensing devices on polymeric substrates. He also worked on the heterogeneous integration of printing and microfabrication technologies for establishing a single fabrication platform. He is recipient of various prestigious scholarships like BK21 (Brain Korea 21st century awards program), Marie Curie Early Stage Researcher Award and ERC Fellow award. He has contributed in more than 40 research articles, five patents and a three Book chapters on nanomaterials based printed sensors.

Shawkat Ali received his masters from National University of Computer and Emerging Sciences, Islamabad, Pakistan, and Ph.D. from Jeju National University, South Korea in 2012, and 2016, respectively, in Electrical/Electronic Engineering. He is currently a postdoc fellow at Hamad Bin Khalifa University, Qatar since 2017. Previously he was serving as Assistant Professor at the department of Electrical Engineering, NU-FAST, Islamabad campus 2016~2017. His areas of interest include Radio Frequency electronics, Nanotechnology, wearable and implantable electronics, biomedical sensors, resistive memory, and energy harvesting. He has been involved in research throughout of his professional carrier and published more than 30 research articles, registered 8 patents and graduated 3 Masters Students. He has been awarded two times as "Productive Scientist" by Pakistan Council for Science and Technology (PCST 2016~2018).

Arshad Khan received his PhD degree in Mechatronic Engineering from the University of Hong Kong (HONG KONG) and a Master's degree in Mechatronic Engineering from Jeju National University, South Korea. He is currently a postdoctoral researcher at College of Science and Engineering, Hamad Bin Khalifa University, Qatar Foundation (Qatar). Previously, he was a joint postdoctoral research fellow between Max Planck Institute for Informatics (MPI-Inf), Germany, and the Leibniz Institute for New Materials (Leibniz-INM), Germany. Dr. Khan's current research focuses on development of self-powered, soft wearable electronics for human activities and health monitoring.

Moaaz Ahmed received the B.S. degree in electrical engineering from the University of Engineering and Technology, Peshawar, Pakistan, in 2007 and double-badged Ph.D. degree in electronic and computer engineering from the Hong Kong University of Science and Technology Hong Kong, and University of Western Australia, Perth, WA, Australia in 2017. Currently, he is a postdoc in the College of Science and Engineering at Hamad Bin Khalifa University, Education City, Doha, Qatar. His research interests include SPICE modeling of CMOS MEMS flow sensors and accelerometers, low-noise instrumentation amplifiers and low-power analog-to-digital converters for sensors readout applications.

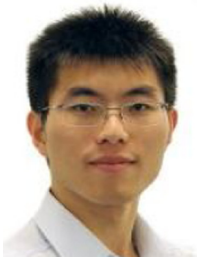

Bo Wang received the B.Sc. degree in the Department of Electrical Engineering from Zhejiang University, Hangzhou, China, in 2010 and the M.Phil degree in the Department of Electronic and Computer Engineering from Hong Kong University of Science and Technology (HKUST), in 2012. He is currently pursuing the Ph.D. degree in the Department of Electronic and Computer Engineering in HKUST. His research interests include smart CMOS temperature sensors and sensor interfaces, on-chip process compensation techniques and heterogeneous sensor integration.

Prof. Amine Bermak received his master's and PhD degrees in electrical and electronic engineering from Paul Sabatier University, France in 1994 and 1998, respectively. He has held various positions in academia and industry in France, the UK, Australia and Hong Kong. Currently, he is a professor in the Information and Computing Technology Division of Hamad Bin Khalifa University. For his excellence and outstanding contribution to teaching, he was nominated for the 2013 Hong Kong UGC best teacher award (for all HK Universities). He is the recipient of the 2011 University Michael G. Gale Medal for distinguished teaching. He is also a two-time recipient of the "Engineering Teaching Excellence Award" in HKUST for 2004 and 2009, respectively. Dr. Bermak has received six distinguished awards, including the "Best University Design Contest Award" at ASP-DAC 2016; "Best paper award" at IEEE ISCAS 2010; the 2004 "IEEE Chester Sall Award"; and the "Best Paper Award" at the 2005 International Workshop on SOC for Real-Time Applications. He has published over 250 articles, designed over 40 chips and graduated 14 Ph.D. and 16 MPhil students. He has served on many editorial boards and is currently the editor of IEEE Transactions on BioCAS and the IEEE TED. Dr. Bermak is a Fellow of IEEE and an IEEE Distinguished Lecturer.